Simulation and analysis of an individual-based model for graph-structured plant dynamics[☆]

F. Campillo[1,*], N. Champagnat[2]

Abstract

We propose a stochastic individual-based model of graph-structured population, viewed as a simple model of clonal plants. The dynamics is modeled in continuous time and space, and focuses on the effects of the network structure of the plant on the growth strategy of ramets. This model is coupled with an explicit advection-diffusion dynamics for resources. After giving a simulation scheme of the model, the capacity of the model to reproduce specific features of clonal plants, such as their efficiency to forage resources and colonize an empty field by means of phalanx or guerrilla strategies, is numerically studied. Next, we propose a large population approximation of the model for phalanx-type populations, taking the form of an advection-diffusion partial differential equation for population densities, where the influence of the local graph structure of the plant takes the form of a nonlinear dependence in the gradient of resources.

Keywords: Markov process, individual-based model (IBM), clonal plant, asymptotic analysis

1. Introduction

Individual-based models (IBMs) are in constant development in computational ecology (DeAngelis and Gross, 1992; Dieckmann et al., 2000; Grimm and Railsback, 2005).

[☆]This work received support by the French national research agency (ANR) within the SYSCOMM project ANR-08-SYSC-012.

[*]Corresponding author

Email addresses: Fabien.Campillo@inria.fr (F. Campillo), Nicolas.Champagnat@inria.fr (N. Champagnat)

[1]Address: MODEMIC project-team, INRIA/INRA, UMR MISTEA, 2 place Viala, 34060 Montpellier Cedex 01, France.

[2]Address: TOSCA project-team, INRIA Nancy – Grand Est, IECN, UMR 7502, Nancy-Université, Campus Scientifique, B.P. 70239, 54506 Vandœuvre-lès-Nancy Cedex, France.

These models aim to represent the dynamics of populations, and in contrast with conventional models where the population is represented as an aggregate state such as the population size or the total biomass, they explicitly describe each individual as well as each mechanism acting on these individuals. In this sense, conventional models correspond to a macroscopic approach and IBMs to a microscopic one. Such a description of an ecosystem at the scale of the individual usually rely on stochastic mechanisms reflecting the interactions of the individual with its neighbors and its environment.

Among plant communities, those involving a clonal reproduction constitute an interesting challenge in terms of modeling. In most clonal plants, growth can be processed horizontally via the development of modified stems, rhizomes or stolons, connecting ramets (Van Groenendael et al., 1996). Ramets are potentially autonomous new individuals and possess aerial and belowground organs in order to sample and uptake resources, like water, light, organic nutrients, nitrates or phosphorus (Van Groenendael et al., 1996; Klimeš et al., 1997). This network structure provides the ability to colonize space (Harper, 1981; Hutchings, 1999), and allows the exchange of resources and information (Marshall, 1990; Stuefer et al., 2004; Wijesinghe and Hutchings, 1997; Hutchings, 1999; Charpentier and Stuefer, 1999; Klimeš et al., 1997). In particular, this network structure implies strong spatial constraints to the architecture of a clonal plant network that have traditionally been classified along a gradient from phalanx to guerrilla strategies (Lovett-Doust, 1981). Phalanx strategies comprise clonal plants with dense network structures with short spacers and resulting in an interrupted front of aggregated ramets with a slow radial propagation (Cheplick, 1997; Humphrey and Pike, 1998). On the contrary, guerrilla strategies produce long and poorly ramified connections which favor space colonization.

The graph structure allows clonal plants to colonize space in order to locate the most favorable areas in terms of resources (spatial colonization sensu Wildova et al., 2007), and exploit the resources in these sites in order to favor the growth of new ramets (potential descendants) in these areas (space occupation sensu Wildova et al., 2007). Spatial structure of the interacting species should be therefore a key element of the dynamics of plant communities.

IBMs generate spatial patterns and dynamics at the scale of plant communities from local interactions between individuals, which are the processes involved in real commu-

nities. A sound model in plant ecology should be spatial and individually based. Two main categories of IBMs can be distinguished: "realistic IBMs" which take into account a large number of mechanisms, and "simple IBMs" which focus on a specific feature of the ecosystem and neglect the others. The first category of models aims for realistic local population structure, whereas the second category can be used to study the influence of a specific feature of the ecosystem on large spatial scales.

For clonal plants, almost all the IBMs studied in the literature belong to the "realistic" category. Most of them are developed on spatial grids (square of hexagonal, for example), representing the possible locations of each element of the plant (Dieckmann et al., 1999; Kun and Oborny, 2003; Oborny, 1994; Oborny et al., 2000, 2001; Oborny and Kun, 2002; Winkler and Klotz, 1997; Winkler et al., 1999; Winkler and Fischer, 2002; Winkler and Stöcklin, 2002). Some models also rely on continuous space domains, where individuals or plant elements can be located at any place in space (Herben and Suzuki, 2002; Herben and Novoplansky, 2008). They belong to a larger class of models, well developed in the more general context of Plant Ecology (Bolker and Pacala, 1999; Dieckmann et al., 1999, 2000; Brown and Bolker, 2004; Bolker, 2004; Fournier and Méléard, 2004; Birch and Young, 2006). Many of these models belong to the class of simple models, because simple IBMs in continuous space and time are within the scope of numerical and mathematical analysis on large spatial scales, whereas IBMs on grids are much harder to study mathematically. These models have originally been developed and studied for adaptive dynamics in evolutionary biology, where plants locations are replaced by individuals' phenotypic quantitative characters (Metz et al., 1996; Dieckmann and Law, 1996; Champagnat et al., 2006; Méléard and Tran, 2009; Champagnat and Méléard, 2011).

IBMs are useful for studying local structures in plant communities, e.g. for development or behavioral studies. However, they are of little practical help for studies at the scale of a field, where one could want to study the competitive exclusion or coexistence of species (Bolker and Pacala, 1999), or simply compute long time statistics of the model, like the mean, equilibrium relative abundance of species. A proficient answer to such questions typically requires us to combine statistical and large time numerical studies, and are hence out of reach of an IBM using usual numerical power (Mony et al.,

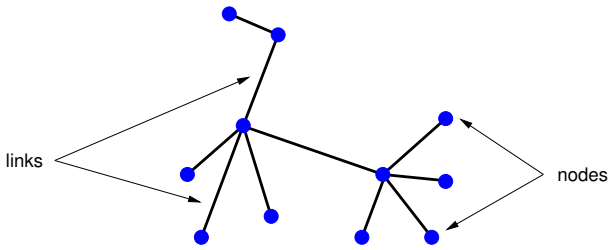

Figure 1: *The plant is represented as a set of nodes connected by links. The nodes can be seen as ramets and the links as rhizomes.*

2012). For such problems, one typically uses partial differential equation (PDE) models (El Hamidi et al., 2012), but usually no aspect of the local architecture of the plants is included in the PDE.

The aim of this work is to construct a simple IBM in continuous space and time for clonal plants, which can be numerically and mathematically studied at the scale of a grassland, and which can make the link between realistic IBMs and PDE models on large scales.

We chose to construct an IBM which focuses on the influence of the graph on the horizontal growth strategy (rate of creation of new connections, new ramets, and the location of new ramets) through a stochastic IBM in continuous time and space, coupled with the graph structure of the plant. In view of the crucial influence of resources exchange between ramets on the space colonization and the localization of favorable areas, we couple our IBM with resources distributed over continuous space, following an advection- diffusion deterministic dynamics. This model is tested in the framework of the phalanx-guerrilla continuum of growth strategies, and we provide exact large population approximations as partial differential equations for the local population density.

2. Dynamics of the plant and of the resources

At time t the clonal plant is represented as a set of nodes (ramets) that may be connected by links (rhizomes or stolons), see Figure 1. In this simplified representation of a clonal plant, ramets are represented by points in the plane, and connection by straight lines between two ramets. All ramets and connections are assumed to be identical

in terms of demographic parameters and resource consumption. Age and growth are neglected, and connections do not uptake resources or incorporate biomass. The influence of other above ground and below ground aspects of the plant are not physically modelled. They are only expressed through the birth and death parameters and the interaction with resources described below.

The state of the nodes is described by the following finite measure:

$$\nu_t = \sum_{i=1}^{N_t} \delta_{x_t^i} \tag{1}$$

where $x_t^i \in \mathbb{R}^2$ is position of the ith node and N_t total number of nodes; δ_x denotes the Dirac measure centered on the point x. The measure ν_t describes the distribution of nodes over the space $\mathcal{D} \subset \mathbb{R}^2$ of spatial positions. We consider for simplicity $\mathcal{D} = [x_{\min}^{(1)}, x_{\max}^{(1)}] \times [x_{\min}^{(2)}, x_{\max}^{(2)}]$. The measure ν_t is a counting measure: $\nu_t(\mathcal{D})$ is the total number N_t of individuals and, for all subdomain B of $\mathcal{D}$, $\nu_t(B) = \sum_{i=1}^{N_t} 1_B(x_t^i)$ is the number of individuals in B.

For any node at position x we define the set of indices of the nodes connected to x:

$$J(t,x) = \left\{ i = 1 \cdots N_t \,;\, x \text{ and } x_t^i \text{ are connected} \right\}. \tag{2}$$

The plant grows in a resource landscape (see Figure 3). At each time t, this resource landscape is represented by $\mathbf{r}(t,x) \in [0, \mathbf{r}_{\max}]$ the available resources at position $x \in \mathcal{D}$. The nodes accessing high levels of resources $\mathbf{r}(t,x)$ are more likely to give birth to new nodes.

Birth and death rates

Each node of ν_t in position x may disappear at a death rate $\mu(t,x)$ and give birth to a new node at a birth rate $\lambda(t,x)$. These rates are *per capita rates*. Global death and birth rates at population level are respectively:

$$\bar{\lambda}_t = \sum_{i=1}^{N_t} \lambda(t, x_t^i)\,, \qquad\qquad \bar{\mu}_t = \sum_{i=1}^{N_t} \mu(t, x_t^i)\,. \tag{3a}$$

The global event rate is:

$$\bar{\mu}_t + \bar{\lambda}_t\,. \tag{3b}$$

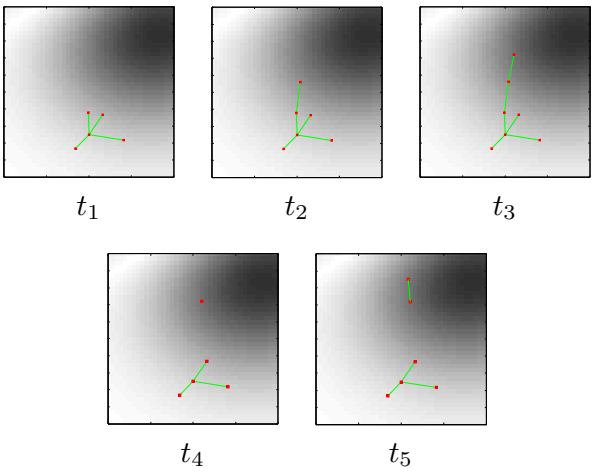

Figure 2: *The nodes evolve in a resource landscape (black/white: high/low resource availability). The nodes accessing high levels of resources are more likely to give birth to new nodes ($t_1 \rightarrow t_2 \rightarrow t_3$). Simultaneously the node and the link between this node and the mother node are created. When a node disappears all the links connected with it simultaneously disappear ($t_3 \rightarrow t_4$).*

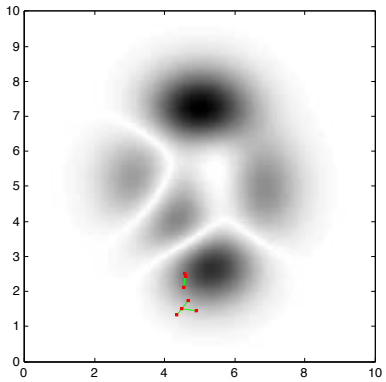

Figure 3: *Snapshot of the resource landscape $\mathbf{r}(t,x) \in [0, \mathbf{r}_{max}]$ at a given time t. The resource dynamics is modeled as an advection/diffusion transport equation* (10) *in interaction with the dynamics of the nodes.*

Basically, the per capita rates depend on the local availability of resources: we suppose that the birth rate $\lambda(t,x)$ is an increasing function of $\mathbf{r}(t,x)$ and the death rate is a decreasing function of $\mathbf{r}(t,x)$. For example:

$$\lambda(t,x) = 1_{\{|J(t,x)|\leq N_{\max}\}} \left(\lambda_0 + \lambda_1 \, \mathbf{r}(t,x)\right), \tag{4a}$$

$$\mu(t,x) = \mu_0 + \mu_1 \left[\mathbf{r}_{\max} - \mathbf{r}(t,x)\right] \tag{4b}$$

where $|J(t,x)|$ is the cardinal of the set $J(t,x)$ and $N_{\max}$ is the maximum number of connections per node. In IBMs on hexagonal grids, one usually has $N_{\max} = 6$ or sometimes less (for example, a ramet never has more than 3 connections in Oborny and Englert, 2012). Note that the continuous space formalism does not require any restriction on the number of connections from a ramet (one could take $N_{\max} = +\infty$). This would lead to more realistic graph structures for sympodial species which display several buds developing from a ramet. Note that the local limitation of resources due to ramet consumption (see below) prevents an excessive local growth of the number of connections and ramets similar to competition processes between plants, and hence implicitely impose a limit on the number of neighbors of each ramet.

When a node is added to the population, it is always linked with the mother node, and the set of connections $J(t,x_t^i)$ corresponding to the mother node and the new node are modified accordingly. In addition, when a node x is removed from population, all connections to x are suppressed from all the sets $J(t,x_t^i)$ (see Figure 2).

Dispersion kernel

We have chosen to focus on the effects of the graph structure of the plant on its horizontal growth strategy, and for simplicity, only on the choice of the position of a new ramet relative to its "father ramet", also called *dispersion kernel*.

A node at position x at time t gives birth to a new node at position $y = x + v$ according to the p.d.f. $D_{t,x}(v)$. We propose the following distribution:

$$D_{t,x}(v) = f(\kappa, (\mathbf{d}_{t,x}, v)) \, g(\|v\|) \tag{5}$$

where

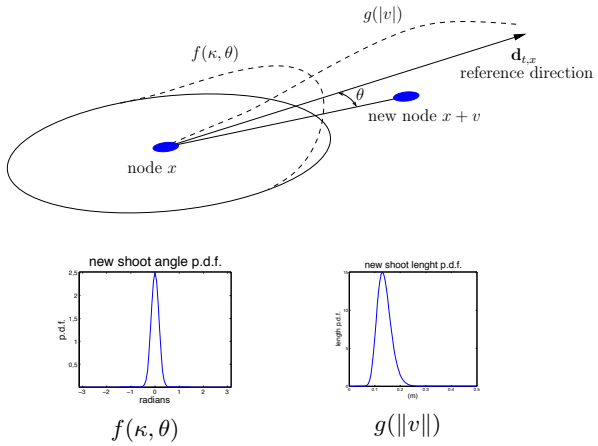

Figure 4: *The dispersion kernel* (5) *is the product of the angle probability density function* f*, the Von Mises distribution, and the length probability density function* g*, the log-normal distribution.*

(i) $(\mathbf{d}_{t,x}, v)$ is the angle between a preferred "direction of reference" $\mathbf{d}_{t,x}$ and the direction of the new shoot v, $f(\kappa, \theta)$ is a p.d.f. on $[-\pi, \pi)$ centered on the angle 0 and with concentration parameter κ. For f we choose the Von Mises distribution (circular normal distribution) with location parameter 0 and a given concentration parameter. The concentration parameter may depend on $\|\mathbf{d}_{t,x}\|$ and when $\|\mathbf{d}_{t,x}\| = 0$, f is chosen as the uniform distribution, i.e. $\kappa = 0$.

(ii) $g(\|v\|)$ is the p.d.f. on the length $\|v\|$ of the connection (see Figure 4); g is chosen as the log-normal distribution.

The preferred direction of reference should capture the effect of the local graph structure of the plant on its horizontal growth. Through their foraging ability, plants are able to explore space and preferentially develop ramets in favorable sites (Van Kleunen and Fischer, 2001), resulting in a preferential directional growth. Such sites could be here sites with the lowest densities of ramets (competitive avoidance sensu Novoplansky, 2009) or sites with the highest resource level. In our model, we assume that growth takes place preferentially in the direction of higher resource level. However, since our model couples plants and resources dynamics, areas with high resource densities and low density of ramets are actually implicitely correlated.

The information about the spatial location of the neighbors of a node at position x

at time t can be summarized by the vector

$$\frac{1}{|J(t,x)|}\sum_{i\in J(t,x)}\frac{x_t^i - x}{|x_t^i - x|}. \tag{6}$$

When there is single neighbor, this vector gives the direction of the connection between the ramets and its "mother ramet". When there are more neighbors, this is simply the mean vector of the directions of each connections leaving the ramet. If one wants to model a preferred direction of growth in unexplored directions, one should favor dispersal in the opposite direction of this vector.

The information about the resource flow entering the ramet at x through connections can be summarized by the (positive or negative) number

$$\frac{1}{|J(t,x)|}\sum_{i\in J(t,x)}[\mathbf{r}(t,x_t^i) - \mathbf{r}(t,x)]. \tag{7}$$

This formula assumes that the flow of resources in a connection is proportional to the resource difference between the two ramets. One could also assume that the flow is proportional to the gradient of resources along the connection, leading to the formula

$$\frac{1}{|J(t,x)|}\sum_{i\in J(t,x)}\frac{\mathbf{r}(t,x_t^i) - \mathbf{r}(t,x)}{|x_t^i - x|}. \tag{8}$$

One could for example assume that the range of dispersal from the ramet is positively influenced by one of these two resource flows.

We have chosen in this work to focus on a compromise between these two effects, based both on positions and resources:

$$\mathbf{d}_{t,x} = \frac{1}{|J(t,x)|}\sum_{i\in J(t,x)}\frac{\mathbf{r}(t,x_t^i) - \mathbf{r}(t,x)}{|x_t^i - x|^2}\,[x_t^i - x]. \tag{9}$$

This is an approximation of the resource gradient based on the values of $\mathbf{r}(t,x)$ at x and at the positions of all connected nodes (see Figure 5).

The way $\mathbf{d}_{t,x}$ approaches $\nabla\mathbf{r}(t,x)$ can be made more precise as follows: using the approximation $\mathbf{r}(t,x_t^i) - \mathbf{r}(t,x) \approx \nabla\mathbf{r}(t,x)\cdot(x_t^i - x)$ for all $i \in J(t,x)$, valid if the connections are short enough, we always have $\mathbf{d}_{t,x}\cdot\nabla\mathbf{r}(t,x) \geq 0$. In addition, in the case where the position of each x_t^i for $i \in J(t,x)$ is uniformly distributed on a circle centered at x (i.e. if $f(\kappa,\theta)$ is the uniform p.d.f. on $[-\pi,\pi)$), a simple computation gives $\mathbb{E}(\mathbf{d}_{t,x}) = \frac{\pi}{2}\nabla\mathbf{r}(t,x)$.

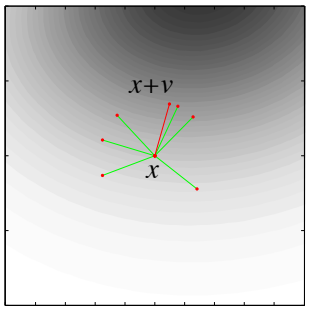

Figure 5: *A node in position x will give birth to a new node in position $x + v$ in an approximation of the gradient of the resources, see* (9).

In order to keep the population inside the domain $\mathcal{D}$ we simply ignore the new node $y = x + v$ when $y \notin \mathcal{D}$.

Interactions between nodes and resources

The natural way to model resource concentration is as a density function $\mathbf{r}(t, x)$ over the domain $\mathcal{D}$. Coupling (discrete) individual dynamics with resource density dynamics is a non-standard problem which requires a choice. We propose the following model:

$$\partial_t \, \mathbf{r}(t,x) = \operatorname{div}\big(\mathbf{a}(x)\, \nabla \mathbf{r}(t,x)\big) + \mathbf{b}(x) \cdot \nabla \mathbf{r}(t,x) - \mathbf{r}(t,x)\, \alpha \sum_{i=1}^{N_t} \Gamma_{x_t^i}(x) \tag{10a}$$

with $\mathbf{r}(0, x) = \mathbf{r}_0(x)$ and

$$\Gamma_y(x) = \exp\big(- \tfrac{1}{2\,\sigma_{\mathbf{r}}^2} \, |x - y|^2 \big) \, . \tag{10b}$$

In the absence of plants, the resource concentration $\mathbf{r}(t, x)$ follows a classical advection/diffusion transport equation. The last term of (10a) represents the resource consumption of the ramets. We assume a rate of resource intake proportional to the local resource concentration during the whole lifetime of each ramet. In addition, we model with the function Γ the fact that resource consumption is not local. The parameter σ_r can then be interpreted as the mean range of roots of a ramet in the species.

The PDE (10) has to be coupled with appropriate boundary conditions. We assume here that the boundary of the domain $\mathcal{D}$ is a natural boundary that cannot be crossed

by the plants, because of the absence of resources. This corresponds to the Dirichlet boundary condition

$$\mathbf{r}(t,x) = 0, \qquad \forall x \in \partial\mathcal{D}\,.$$

Of course, other resource consumption models can be considered. For example, consumption can be assumed to occur also at birth, leading to the following resource update at a birth of a ramet at position y and time t:

$$\mathbf{r}(t,x) = \mathbf{r}(t^-,x)\,\big(1-\alpha'\,\Gamma_y(x)\big)\,.$$

One could also take into account the degradation of plants at position y after its death at time t by updating the resource concentration according to

$$\mathbf{r}(t,x) = \mathbf{r}(t^-,x)\,\big(1+\alpha''\,\Gamma_y(x)\big)\,,$$

which corresponds to an instantaneous degradation of the plant.

3. Numerical approximation of the IBM

We now describe the simulation algorithm: starting from the state

$$\nu_{T_{k-1}} = \sum_{i=1}^{N_{T_{k-1}}} \delta_{x^i_{T_{k-1}}}$$

at last event time T_{k-1}, we first sample the time of the next event (birth or death):

$$T_k = T_{k-1} + S \qquad \text{with} \quad S \sim \mathrm{Exp}\big(\bar\lambda_{T_{k-1}} + \bar\mu_{T_{k-1}}\big) \tag{11}$$

and $\bar\lambda_{T_{k-1}}$ and $\bar\mu_{T_{k-1}}$ defined by (3a). The next event:

- is a birth event with probability

  $$\bar\lambda_{T_{k-1}}/(\bar\lambda_{T_{k-1}} + \bar\mu_{T_{k-1}})\,.$$

  Then sample î according to

  $$\{\lambda(T_{k-1}, x^i_{T_{k-1}})/\bar\lambda_{T_{k-1}}\,;\, i = 1,\dots,N_{T_{k-1}}\}$$

  and v according to the p.d.f. $D_{T_{k-1},x^{\hat\imath}_{T_{k-1}}}(v)$, finally let:

  $$\nu_{T_k} = \nu_{T_{k-1}} + \delta_{\left(x^{\hat\imath}_{T_{k-1}}+v\right)}$$

  and update the sets of connections $J(T_k,x)$ accordingly;

- is a death event with probability

$$\bar{\mu}_{T_{k-1}}/(\bar{\lambda}_{T_{k-1}} + \bar{\mu}_{T_{k-1}})\,.$$

  Then sample î according to

$$\{\mu(T_{k-1}, x^i_{T_{k-1}})/\bar{\mu}_{T_{k-1}}\,;\, i = 1, \ldots, N_{T_{k-1}}\},$$

  let:

$$\nu_{T_k} = \nu_{T_{k-1}} - \delta_{x^{\hat{\imath}}_{T_{k-1}}}$$

  and update the sets of connections $J(T_k, x)$ accordingly.

Note that this algorithm is valid if the rates $\lambda(t, x^i_t)$ and $\mu(t, x^i_t)$ are approximately constant for $t \in [T_{k-1}, T_{k-1} + S)$. If it is not the case, we should make use of an acceptance/rejection algorithm (Fournier and Méléard, 2004; Campillo and Joannides, 2009). In parallel, we should numerically integrate the PDE (10), for example with implicit or explicit finite-difference schemes. In practice, if $T_k - T_{k-1}$ is small enough, which is usually the case if the population is large, a single time step of the finite-difference scheme is sufficient. Note also that, in order to compute the birth and death rates λ and μ, one needs to interpolate the resource concentration at each ramet position from the resource concentrations on the discretization grid. The algorithm is presented in Algorithm 1.

Because the model contains no grid structure, this algorithm is particularly simple to implement. The state of the process can be coded as a list of each individual's location and the labels of its neighbors.

Note also that this algorithm can be very costly when the population size is large, as it requires us to compute the sums $\bar{\lambda}$ and $\bar{\mu}$ at each time step. Another possibility is to use an acceptance/rejection procedure (Fournier and Méléard, 2004) in order to replace this sum by a random sampling of the individual to which the next event will apply. The drawback is that some (and sometimes many) of these events may actually be void, leading to an increase of the number of time steps in the simulation. In practice, there is a significant gain of numerical cost for very large populations.

$T_0 \leftarrow 0$, ν_0, $\mathbf{r}(0,x)$ given
for $k = 0, 1, \ldots$ **do**
  compute the rates $\lambda(T_k, x)$, $\mu(T_k, x)$, for $x \in \nu_{T_k}$
  $\bar{\lambda} \leftarrow \sum_{x \in \nu_{T_k}} \lambda(T_k, x)$, $\bar{\mu} \leftarrow \sum_{x \in \nu_{T_k}} \mu(T_k, x)$
  $T_{k+1} \leftarrow T_k + S$ with $S \sim \mathrm{Exp}(\bar{\lambda} + \bar{\mu})$
  if `rand()` $< \bar{\lambda}/(\bar{\lambda} + \bar{\mu})$ **then**
    sample x according to $\{\lambda(T_k, x)/\bar{\lambda}; x \in \nu_{T_k}\}$
    sample v according to $D_{T_k,x}(v)$
    $\nu_{T_{k+1}} \leftarrow \nu_{T_k} + \delta_{x+v}$ [birth]
  else
    sample x according to $\{\mu(T_k, x)/\bar{\mu}; x \in \nu_{T_k}\}$
    $\nu_{T_{k+1}} \leftarrow \nu_{T_k} - \delta_x$ [death]
  end if
  compute $\mathbf{r}(T_{k+1}, x)$ [numerical approximation of (10)]
end for

Algorithm 1: *Gillespie algorithm. Here we use the notation $x \in \nu_t$ instead of x^i for $i = 1 \cdots N_t$.*

4. Simulation

We simulated through this model the growth of two contrasted growth forms: guerrillas and phalanx growth strategies (sensu Lovett-Doust, 1981) in a heterogeneous resource concentration landscape. We implemented both types by suitably adjusting the parameters of the dispersion kernel in (5):

(i) if the p.d.f. $f(\kappa, \theta)$ of the shoot angle has a large concentration parameter and if the p.d.f. $g(\|v\|)$ favors large lengths, then the model will present the characteristics of a guerrilla plant;

(ii) if the p.d.f. $f(\kappa, \theta)$ of the shoot angle has a small concentration parameter and if the p.d.f. $g(\|v\|)$ favors small lengths, then the model will present the characteristics of a phalanx plant;

see Figure 6. Examples of resulting plant networks are presented in Figure 7 for the case of a maximum number of $N_{\max} = 3$ connexions per node.

These preliminary simulation tests are run for very simple dynamics of resources: we assume that there is no advection of resources over the land ($\mathbf{b}(x) = 0$) and that the diffusion coefficient of resources is constant ($\mathbf{a}(x) = \sigma^2$) in (10a). Since the colonization

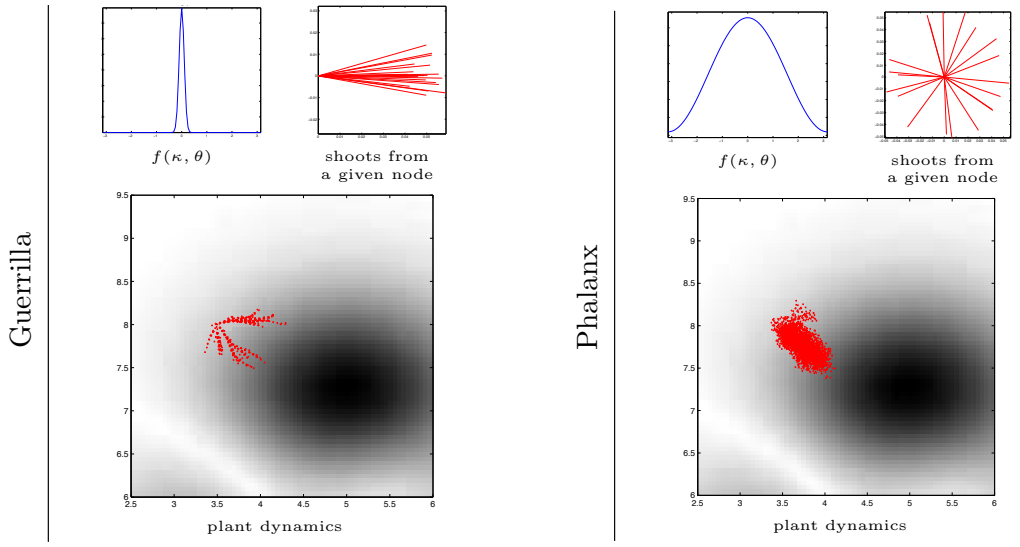

Figure 6: *If the shoot angle p.d.f. $f(\kappa, \theta)$ has a small concentration parameter κ (resp. large concentration parameter κ) and if the p.d.f. $g(\|v\|)$ favors small lengths (resp. large lengths), then the model will present the characteristics of a phalanx growth strategy (resp. guerrilla growth strategy).*

occurs on a short time-scale, we also neglect the degradation phenomenon by which resources return to the environment. The resource landscape is chosen multimodal: the resources are distributed in several patches. Our goal is to test the capabilities of our clonal plant model to explore space and to adapt its network according to the distribution of resources.

For the phalanx strategy, we observe a dense colonization front, because of the excess of resources. Away from the front, the population density stabilizes to a lower level, due to the stabilization of the resource concentration at a small level. For the guerrilla strategy, the colonization front is not as clearly delimited, but we still observe an area with high density where the colonization progresses, and the stabilization of resources and population densities in already colonized regions.

One of the main advantages that network structure are believed to confer to clonal plants is their capacity to adapt their growth strategy to the local resources landscape, felt either by foraging or physiological integration. This capacity is given in our IBM by the dependency of the dispersion kernel – more precisely the shoot angle p.d.f. f – on the estimated resource gradient $\mathbf{d}_{t,x}$ (9).

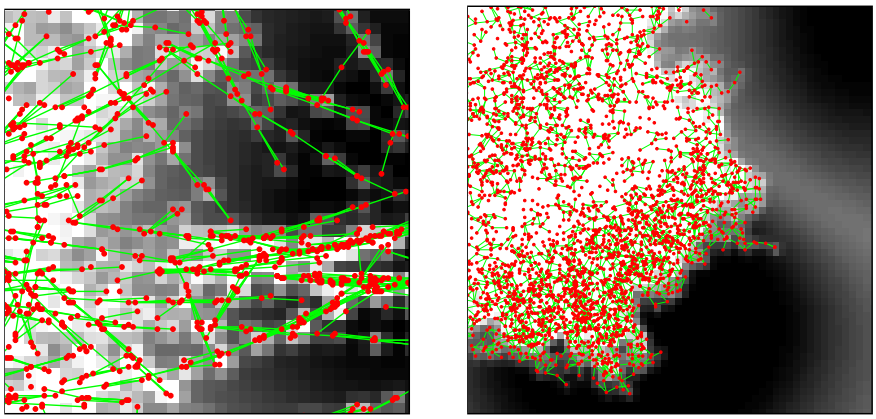

Figure 7: *Simulation of guerrilla and phalanx behavior descried in Figure 6 with a maximum number of* $N_{max} = 3$ *connections, see* (4a).

The efficiency to exploit resources can then be compared with simulations of IBM involving different dispersion kernels. This is done in Figure 8 with the initial resource landscape given by Figure 3.

This resource map features several resource-rich areas (patches), with different levels of resource richness, separated by resource-poor areas of different width. The arbitrary choice we made is intended to provide various situations to test the ability of the clonal plant to (i) cross areas with small resource density in order to visit new patches and (ii) to uptake resources within a patch efficiently.

Pure guerrilla strategies are efficient for the first point (because the plant grows along straight lines), but inefficient for the second point. Pure Phalanx strategies are less efficient for the first point, but more efficient for the second point (as they grow in all directions).

We explore a range of intermediate strategies simply by varying the concentration of the shoot angle distribution f. A large concentration means that the plant grows nearly along straight lines and has a very small probability to change its growth direction. A small concentration corresponds to the case where the graph structure has no influence on the population dynamics, i.e. the case where f is the uniform distribution on $[0, 2\pi)$.

As expected, the simulations of Figure 8 show that there is an optimal tradeoff: when the shoot angle p.d.f. is not directive enough or too directive, the plant fails to reach areas with high level of resources; in intermediate cases, the plant reaches these areas and reaches them rapidly.

5. Large population approximation of the IBM

Individual-based models are a convenient tool for modelling small-scale ecological systems. However, their simulation is often costly and can hardly provide relevant field-scale information in reasonable computational time. This is typically the case for phalanx-type clonal plants, where the connection length is often short and the plant architecture is dense. In order to understand the global interaction between plants and resources and to speed up the computational time, the search for simpler approximation models is crucial.

It is natural to seek partial differential equations (PDE) (El Hamidi et al., 2012) governing the time dynamics of the population density over space, obtained in a limit of large population. This has been done under various scalings of the individual parameters for plants systems without network structure (Fournier and Méléard, 2004; Champagnat et al., 2006, 2008). Three main families of scalings were described in the second paper: in the first scaling, space is unscaled, leading to a *non-local* integro- differential equation for the population density; in the second one, space is scaled, and births and deaths are accelerated accordingly in order to obtain a PDE with *local* reaction-diffusion; in the last scaling, births and deaths are even more accelerated, leading to a *stochastic* reaction-diffusion PDE.

Because of the underlying network structure and the explicit coupling with resource dynamics, these results do not apply to our IBM. The result we present here is a first attempt to fill this gap. This is a convergence theorem under appropriate parameter scalings, so we insist on the fact that the limit is *exact*. We give in the Appendix an argument justifying this convergence, but we do not provide a full proof, which would be very technical because our model couples a stochastic, discrete structure for the population and a deterministic, continuous structure for resource concentrations (see Campillo and Champagnat, 2012, for a proof in a graph-structured IBM without resources).

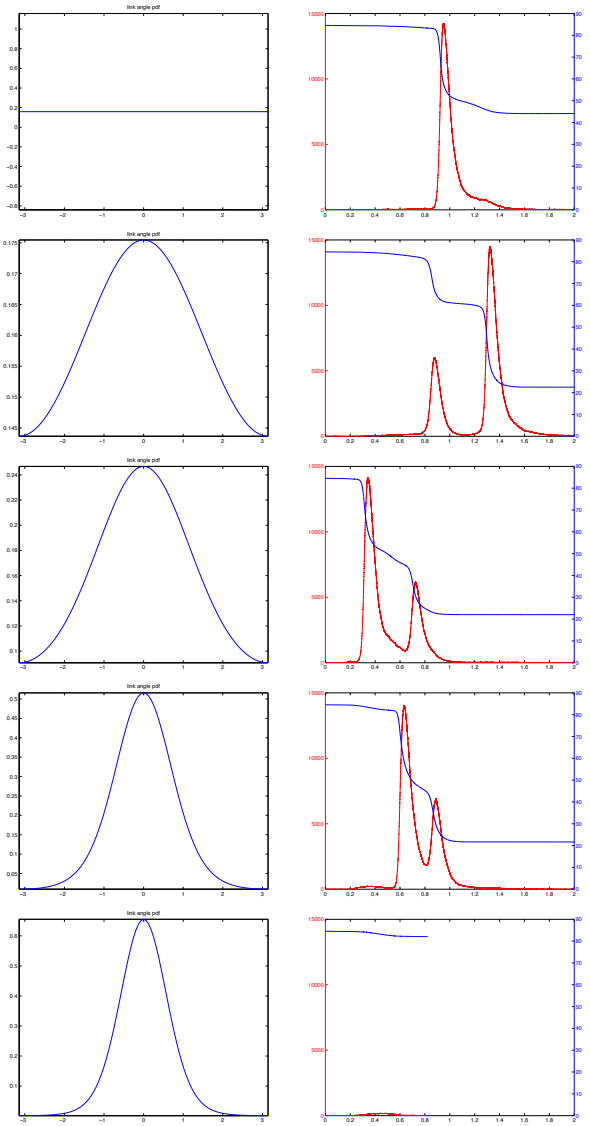

shoot angle p.d.f. $f(\theta)$ *evolution of the population size (red) and of the amount of resources (blue)*

Figure 8: *Let κ be the concentration parameter of the Von Mises distribution f. Taking different values for this parameter ($\kappa = 0$, 0.1, 0.5, 2, 3) we plot, on the left, the corresponding shoot angle p.d.f. $f(\kappa, \theta)$ and, on the right, the time evolution of the size of the population (red) and of the total resource (blue); we suppose that there is no advection of resources (i.e. $\mathbf{b} \equiv 0$ in (10)). The simulation is done with the initial resource map of Figure 3 with high resources spot on the north of the domain, a less important spot in the south and 3 negligible spots (left, center and right), the initial plant is located on the left spot. In the first case, $\kappa = 0$, the plant explore all directions without any preference (uniform distribution of the shoot angle): by chance the plant reaches the north spot corresponding to the increase of population and the population subsequently decreases. In the second case, $\kappa = 0.1$, the plant first reaches the south spot and then the north spot. In the third case, $\kappa = 0.5$, the plant rapidly reaches the north spot and then the south spot. In the fourth case, $\kappa = 2$, the plant needs more time to reach the two important spots. In the last case, the plant does not reach any resource spot and node population goes extinct rapidly.*

The limit PDE

The more relevant scaling within the context of phalanx-type clonal plants is the space-scaling and acceleration of births and deaths which leads to a reaction-diffusion PDE for population densities. It is also the less technical, and we restrict ourselves to this case here. Other possible scalings are discussed below (see also Campillo and Champagnat, 2012). In this case, the PDE approximation of the IBM takes the following form: denoting by $u(t,x)$ the population density at time t and position x in $\mathcal{D}$,

$$\begin{cases} \partial_t u(t,x) = \beta\,\Delta(\gamma(x)\,u(t,x)) + (\lambda(t,x) - \mu(t,x))\,u(t,x) \\ \qquad\qquad\qquad\qquad -\mathrm{div}(\gamma(x)\,F(x,\nabla \mathbf{r}(t,x))\,u(t,x))\,, \\ \partial_t \mathbf{r}(t,x) = \nabla(\mathbf{a}(x)\,\mathbf{r}(t,x)) + \mathbf{b}(x)\cdot\nabla\mathbf{r}(t,x) \\ \qquad\qquad\qquad\qquad -\delta\,\mathbf{r}(t,x)\,u(t,x), \\ u(t,x) = \mathbf{r}(t,x) = 0, \qquad\qquad \forall x \in \partial\mathcal{D}. \end{cases} \tag{12}$$

This model is a diffusion-advection PDE for population densities with a term of local growth, coupled with an diffusion-advection PDE for resources, where the resource consumption depends on the local population density $u(t,x)$ and the advection of the population density depends on the local gradient of resources $\nabla\mathbf{r}(t,x)$. Note that the PDE for u is linear, but depends non-linearly on $\mathbf{r}$ through F, λ and μ. Therefore, this is not strictly speaking a reaction diffusion PDE as in the competition-colonization plant model of Champagnat et al. (2006). Note also that the local growth rate of the population density is given as one could expect by $\lambda(t,x) - \mu(t,x)$.

The parameters β, γ, δ and F appearing in this equation are obtained as explicit functions of individual parameters in the Appendix.

The parameter scalings

The PDE (12) is obtained from a large population scaling of our IBM. Hence, we introduce a parameter K which will give the order of the total number of individuals in the population. The constant K is related to the carrying capacity of the system and is also often called "system size" (Metz et al., 1996). We also fix a parameter $\eta \in]0,1[$. We denote by ν^K and $\mathbf{r}_K$ the population measure and resource concentration corresponding

to the parameter K, and we scale ν^K as

$$\nu_t^K = \frac{1}{K}\sum_{i=1}^{N_t^K} \delta_{x_t^i}.$$

First, in order to make the population larger, we need to increase the quantity of resources available, or equivalently to reduce the rate of resource consumption per individual:

$$\partial_t\, \mathbf{r}_K(t,x) = \mathrm{div}\big(\mathbf{a}(x)\,\nabla \mathbf{r}_K(t,x)\big) + \mathbf{b}(x)\cdot\nabla \mathbf{r}_K(t,x) - \frac{\alpha}{K}\,\mathbf{r}_K(t,x)\sum_{i=1}^{N_t^K}\Gamma_{x_t^i}^K(x), \qquad (13)$$

which amounts to replacing α by α/K in (10). We also apply a space scaling, which corresponds to the choice

$$\Gamma_y^K(x) = K^{-\eta/2}\exp\big(-\tfrac{K^\eta}{2\,\sigma_{\mathbf{r}}^2}\,|x-y|^2\big)\,.$$

in the resource dynamics. This means that the typical size of a ramet (and its roots, stolons excluded) is of order $K^{-\eta/2}$ in the new space-scale. Since the integral of Γ_y^K over space remains of order 1, the total amount of resources consumed per ramet and per unit of time remains of order $1/K$ (because α has been divided by K). This is consistent with a total population size of order K.

Concerning the population dynamics, we require that births and deaths are accelerated as follows:

$$\begin{aligned} \lambda_K(t,x) &= \lambda(t,x) + K^\eta\,\gamma(x), \\ \mu_K(t,x) &= \mu(t,x) + K^\eta\,\gamma(x), \end{aligned} \qquad (14)$$

where λ and μ may depend on $\mathbf{r}$ as in (4). This means that, while keeping the growth rate per individual $\lambda_K - \mu_K = \lambda - \mu$ constant, births and deaths are accelerated by the term $K^\eta\gamma$, where γ is a function that may depend on $x \in \mathcal{D}$. This corresponds to a time-scale where ramets have short life spans and reproduce rapidly, while the total population grows or declines on a slower time scale. In other words, we want to describe the global changes in the population on an intermediate time scale, after the initial (fast) colonization of space, but before it stabilizes to a global equilibrium.

Finally, the space scaling must also be applied to the dispersion kernel, and the preferred dispersion direction must be consistent with the phalanx-type population we consider: we replace the dispersion distribution of (5) by

$$D_{t,x}^K(v) = \frac{1}{K^\eta}\,g\Big(\frac{\|v\|}{K^{\eta/2}}\Big)\Big((1-K^{-\eta/2})\frac{(\mathbf{d}_{t,x},v)}{2\pi} + K^{-\eta/2}\,f(\kappa,\,(\mathbf{d}_{t,x},v))\Big). \qquad (15)$$

The scaling of the p.d.f. g corresponds to the space scaling of $K^{-\eta/2}$ which was used above for the resource consumption kernel Γ^K. The scaling of the p.d.f. f amounts to a uniform dispersion direction with probability $1 - K^{-\eta/2}$ and otherwise to a dispersion direction around the preferred direction according to f. This corresponds to a population with nearly no preferred direction, hence a phalanx-type population. Still, the small probability $K^{-\eta/2}$ for a dispersal along the preferred direction has an effect at large space-scales on the global behavior of the population, corresponding to the term $F(x, \nabla \mathbf{r}(t, x))$ in the limit PDE (12). This shows that even a small asymmetry in the dispersal direction for each ramet can lead to a non-negligible global effect. Again, this global effect can be explicitly expressed in terms of the individual parameters (see Appendix).

6. Discussion

The construction of a model in any scientific domain has to meet several contradictory goals and must often be a compromise. The first goal is of course the faithfulness of its results compared to the quantitative results of experiments, and as a consequence, the details and precision that the model should include in all the relevant mechanisms. The second goal is its practical interest in terms of prediction, description and analysis of the phenomenon under study. In this respect, we can distinguish several major issues: the number of parameters of the model, the difficulty of its numerical implementation, the numerical cost of its simulation and the possibility of its mathematical analysis. The tendency to build complicated models to describe natural phenomena has to be faced with the problems of calibration of too many parameters compared with the amount of data available, the arbitrary choices that must often be made in the details of the model, and the numerical cost of its simulation, which can make statistical information or large time behaviors out of reach.

The construction of a useful model requires to restrict to the significant factors involved in the phenomenon. Of course, the notion of significant factors is highly dependent of the goals of the study. In Ecology, depending on the spatial scale of the study, one may prefer to use "realistic IBMs" which aims to describe realistic local population structures, or "simple IBMs" which focus on a specific feature of the ecosystem and can be used to study its influence on large space scales. For clonal plants, the first class of models

has received much more attention than the second one, and this work is an attempt to construct a simple IBM for clonal plants which can be numerically and mathematically studied at the scale of a grassland.

A simple IBM allowing to simulate the growth of two clonal plants

In this work, we presented a simple IBM for clonal plants in continuous time and space, which can be numerically and mathematically studied on large space-scale. To this aim, we chose a modelling compromise which consists in substantially simplifying several aspects of the local architecture of the plant, while focusing on a single aspect: the influence of the graph structure of the plant on its horizontal growth strategy. Our goal was to model the influence of the network structure of the plant on its ability to colonize space (Harper, 1981; Hutchings, 1999) through the exchange of resources and information along connections (Marshall, 1990; Stuefer et al., 2004; Wijesinghe and Hutchings, 1997; Hutchings, 1999; Charpentier and Stuefer, 1999; Klimeš et al., 1997). This was done by constructing a preferred horizontal growth direction based on the position and resources of the neighbors of a ramet in the network. This preferred growth direction influences the position of new ramets. Because of the importance of resources in the horizontal growth strategy, we also included an explicit resource dynamics in the model taking the form of an advection-diffusion partial differential equation.

Typical network architectures of clonal plants range from phalanx to guerrilla strategies (Lovett-Doust, 1981). These strategies strongly influence the horizontal growth of clonal plants, which in turn strongly influences their colonization and space occupation abilities (Wildova et al., 2007). Based on a partly exact simulation scheme, as the exact IBM scheme is coupled with an approximate resources dynamics, the numerical study of our IBM was done in the context of the colonization of a land with an heterogeneous and fragmented resource landscape. We proposed a possible parameterization of guerrilla and phalanx strategies in our model, and we studied the efficiency of these strategies on the speed of colonization and the resource consumption.

We observed a trade-off between exploration and exploitation inducing contrasted colonization performance of plants. Space colonization depended on the species clonal dispersal strategy. Guerilla species were the most efficient at exploring space as their strategies enable them to colonize space and minimize competition within the clone

(Lovett-Doust, 1981). These differences in the success of these two strategies are consistent with previous studies (Humphrey and Pike, 1997).

The average distance between two connected ramets and the variance of the gap between the actual and the preferred directions of growth appear to be particularly important traits for the plant efficiency. In our simple situation, we observed the existence of an optimal resource consumption, intermediate between pure phalanx and pure guerrilla strategies. The importance of architectural trait in plant performances has been a key question in clonal plant studies, especially studied through modelling approaches (Winkler and Schmid, 1995; Wildova et al., 2007; Wong et al., 2011). In particular, angles between branches have been shown to be a key element for determining the ability of a plant to handle the trade-off between intraclonal competition and space colonization (Bell, 1979; Kisljuk et al., 1996; Wong et al., 2011). The model of Smith and Palmer (1976) demonstrated that a hexagonal architecture would maximize the centrifugal spread and area colonized by the clonal fragment, while generating gaps within it. Weak variation of this angle disfavors ramet superposition (Bell and Tomlinson, 1980).

Comparison with other classes of IBMs

IBMs on a grid are a convenient way to model the spatial constraints on the network structure of a plant community without giving too much care to the underlying mechanisms. For example, a spatial grid limits the local spatial density of ramets or spacers, and the complexity of the network structure. This is probably an important reason for the success of IBMs on grids for clonal plant modelling.

However, IBMs on grids also have some drawbacks: they can produce unrealistic structures of the plant (particularly for sympodial species), the spatial constraints are modelled in an arbitrary way, the numerical implementation of the model can be complex due to the grid structure, and the models can be analyzed only via simulations.

IBMs in continuous space can answer several of the above mentioned drawbacks: the absence of grid can solve the spatial artifacts of IBMs with grid; the spatial constraints can be modelled as a direct consequence of the interaction between plants and resources; the numerical implementation of the model is very simple and its numerical cost is good (Section 3); finally, provided they are not too complicated, these models are amenable to *exact* macroscopic approximations (Section 5).

However, IBMs in continuous space also have drawbacks, among which: (i) the graph-structure of the plant can be unrealistic, since a ramet can produce two very close new ramets or the local ramet density could be very high; (ii) it is harder to include a realistic interaction between ramets and resources, since resource concentrations are modelled as continuous variables over continuous space, whereas individuals are discrete. This last point is a major difficulty, since the structure of the root system, the mechanisms of resource absorption by roots (including stolons) and the degradation of the plants are very complex. We proposed a simple solution for this problem, probably unrealistic. Still, one can hope that differences on the resource consumption mechanisms at the local scale have a small influence on larger space-scale. This is supported by our mathematical analysis in the Appendix, where the resource consumption profile of (10b) only influences the global dynamics of the population through its mass and its standard deviation σ_r. To our knowledge, the mechanism of resource consumption which we use is the first one proposed in the context of a discrete population and a resource landscape over a continuous space.

Our model belongs to the family of "simple IBMs": the basic elements of the plants are ramets and connections between ramets (rhizomes or stolons), and the above ground and below ground aspects of the plant are not physically modelled. Of course, this makes the model unrealistic concerning the local architecture of the plant. However, our simulations show that our model is able to capture global features of the horizontal growth of plants, such as guerrilla or phalanx growth strategies.

In addition, our model has a much smaller number of parameters than traditional IBMs for clonal plants (5 parameters for birth and death rates: the minimal and maximal birth and death rates and the maximum number of neighbors; 4 parameters for the dispersal kernel). This makes our model much easier to calibrate than models giving more details to the plant structure. One of the most promising approaches to calibrate IBMs lies in the approximate Bayesian computation method (Hartig et al., 2010).

Our purpose was to construct a simple IBM that can be mathematically analized. However, "realistic IBMs" are a key tool for studying local structures in plant communities, e.g. for development or behavioral studies. We can propose various extensions of our model for future studies: (i) to account for unsuccessful exploration of space by the

stolon, one can add to the model a probability of actual birth of a new ramet, which could depend on the local resource concentration; (ii) the birth and death rates (4) may also depend on resource translocation between ramets (Stuefer et al., 2004), for example through incoming flow like those defined in (7) or (8); (iii) one can consider external supply of resources, either with flux (Neumann) boundary conditions or source terms for the resources PDE (10a); (iv) more generally all information on the plant architecture usually included in realistic IBMs could be easily translated in models on continuous space. For example, one can attach variables to each ramet, like their size, age or biomass (for example, resources attached to a ramet sensu Herben and Novoplansky, 2008), and let the birth and death parameters depend on these variables. Internal or terminal ramets could also be distinguished (Oborny and Englert, 2012). Spacers can also disconnect at a given rate (Herben and Novoplansky, 2008), be characterized by an amount of resources or biomass (physiological integration sensu Stuefer et al., 2004), or grow linearly in continuous time, similarly as in most of the IBMs of clonal plants on grids.

Towards PDE models for various types of clonal plants

We proposed a PDE model which approaches the IBM when the population is large, the births and deaths are fast and the size of ramets and spacers is small. This particular scaling is relevant for clonal plants with phalanx strategies on large space-scales.

The derivation of such a result is usually only possible for "simple IBMs", and much easier for IBMs in continuous space. For particle systems on grids, similar results exist, but usually under mixing assumptions (hence their name of hydrodynamic limits), like fast motion of individuals (Durrett, 1995; Kipnis and Landim, 1999). Unfortunately, such assumptions are totally irrelevant for IBMs of plant dynamics. The difficulty comes from the fact that, without mixing assumptions, IBMs on grids remain influenced by the geometry of the grid on large space scales (a celebrated example in a different context is the Wulff crystal shape in statistical mechanics, see Cerf, 2006).

In the class of simple IBMs in continuous space, the first macroscopic results were obtained using moment equations and their approximation by closure methods under various space scalings (Bolker and Pacala, 1999; Dieckmann et al., 1999, 2000; Brown and Bolker, 2004; Bolker, 2004). Afterwards, these results were improved with exact convergence results to PDEs for population densities, using large space-scale and large

population asymptotic (Fournier and Méléard, 2004; Champagnat et al., 2006; Campillo and Joannides, 2009; Méléard and Tran, 2009). All these results were obtained in models without network structure.

Our method, which makes the connection between IBMs with graph structure in continuous space, and continuous PDE models, is new and shows how the local details of the model can keep a non-trivial influence at larger space-scales. In addition, it can be extended to other scalings of our IBM in the fashion of Champagnat et al. (2008) and Campillo and Champagnat (2012), or to more complex interactions: (i) the birth, death and dispersion parameters may also depend on the mean position of the neighbors of a ramet (6) or on the flow of resources (7) or (8) entering a ramet; (ii) one can also scale the population size without scaling space, by taking $\eta = 0$ in Section 5; in the limit, the population densities solve a non-local PDE (as the network is unscaled), and must be expressed also as a function of the age and parent position of a randomly sampled individual (Campillo and Champagnat, 2012); (iii) our scaling can also be applied to guerrilla-type strategies, for which the preferred growth direction has a strong influence; in this case, the limit population density solves a *pure advection* (or *transport*) PDE, of very different nature than the reaction-diffusion PDE obtained for phalanx strategies in Section 5; (iv) one can also handle the case $\eta = 1$, where some demographic stochasticity remains in the limit of large population, in the fashion of the Fleming-Viot process (Etheridge, 2004; Champagnat et al., 2006).

Conclusion

By voluntary limiting ourselves to a simple individual-based model, we were able to propose a precise asymptotic analysis that allowed us to approximate, at the scale of the field, the IBM by a PDE system. This work is the first result that bridges the gap between IBM and PDE in the context of clonal plant growth.

This scaling is especially valid for clonal plants with phalanx-type growth. Other scalings can also be considered for guerrilla-type populations. This is an interesting perspective in terms of competition models between two species of clonal plants competing for common resources. Depending on the scale of study or the species, it could be pertinent to consider hybrid models, where one species could be modelled in PDE terms and the other species could be modelled in IBM terms.

We believe that the dual representation of IBMs, by means of computer simulation tools and of mathematical formalisms, will greatly expand in the future.

Appendix — Approximation argument for the limit PDE (12)

Equation (12) can be derived from the scaling described in Section 5 as follows: we assume that the initial population state ν_0^K converges to some non-trivial measure $u_0(x)dx$ on $\mathcal{D}$, i.e. that the initial population size is of order K and is distributed over space close to the population density $u_0(x)$. Now, assume that K is large and that at some time t, the population state ν_t^K is close to the density $u(t,x)$, and consider some test function ϕ over $\mathcal{D}$. Then, the quantity $A_t = \int_D \phi(x)\,\nu_t^K(dx)$ changes on the time interval $[t, t+dt]$ due to the following three effects:

- Each individual close to $x \in \mathcal{D}$ gives birth to a number $\lambda_K(t,x)\,dt$ of individuals, and a proportion $\mu_K(t,x)\,dt$ die. This gives a local change of the population density $(\lambda_K(t,x) - \mu_K(t,x))\,u(t,x)\,dt$, and a change of A_t given by

$$\int_D \phi(x)\,(\lambda(t,x) - \mu(t,x))\,u(t,x)\,dx\,dt.$$

  This gives the first-order change of A_t. Higher-order changes (i.e. changes involving derivatives of ϕ) must also be taken into account.

- Among all the births from the individuals around $x \in \mathcal{D}$, a proportion $1 - K^{-\eta/2}$ are located symmetrically around x at a distance $K^{-\eta/2}\,\rho$, where ρ is distributed as $g(\rho)$. Making a Taylor expansion of ϕ around x, the corresponding change of A_t is given by

$$dt \int_D dx\,\lambda_K(t,x)\,u(t,x) \int_0^{2\pi} \frac{d\theta}{2\pi} \int_0^{+\infty} g(\rho)\,d\rho \times \frac{1}{2}\,(\rho\,K^{-\eta/2}\,v_\theta)'\,\nabla^2\,\phi(x)\,(\rho K^{-\eta/2}\,v_\theta),$$

  where $v_\theta = (\cos\theta, \sin\theta)$ is the unit vector of direction θ. Note that the first-order term does not appear as it vanishes because of the symmetry of dispersions. Note also that the scaling of λ_K in (14) has been chosen so that it exactly cancels the scaling of the dispersion distance $K^{-\eta/2}\rho$. Neglecting the smaller order terms, an

easy computation gives a change of A_t of

$$\frac{\int_0^{+\infty} \rho^2\, g(\rho)\, d\rho}{4} \int_D \Delta\, \phi(x)\, \gamma(x)\, u(t,x)\, dx\, dt.$$

- Among all the births from the individuals around $x \in \mathcal{D}$, a proportion $K^{-\eta/2}$ are located at $x + K^{-\eta/2} v$, where v has distribution (5). Making again a Taylor expansion of ϕ, we obtain a local change of A_t of

$$dt \int_D K^{-\eta/2} \lambda_K(t,x)\, u(t,x)\, \nabla\phi(x) \cdot K^{-\eta/2} \langle v_{t,x} \rangle\, dx,$$

  where $\langle v_{t,x} \rangle$ is the mean of $v_{t,x}$ when v has distribution (5), in which $\mathbf{d}_{t,x}$ has the distribution of the preferred dispersion direction in the population around x. Of course, this last distribution is unknown and must be computed (see below).

Putting together all the previous results, we obtain

$$\frac{dA_t}{dt} = \int_D \Big(\tfrac{\int_0^{+\infty} \rho^2\, g(\rho)\, d\rho}{4}\, \Delta\phi(x)\, \gamma(x)\, u(t,x) + \phi(x)\, (\lambda(t,x) - \mu(t,x))\, u(t,x) + \nabla\phi(x)\, \langle v_{t,x} \rangle\, \gamma(x)\, u(t,x) \Big)\, dx\,.$$

This is the weak formulation of the PDE (12), where we put

$$\beta = \frac{\int_0^{+\infty} \rho^2\, g(\rho)\, d\rho}{4},$$
$$F(x, \nabla \mathbf{r}(t,x)) = \langle v_{t,x} \rangle.$$

The fact that $\langle v_{t,x} \rangle$ only depends on x and $\nabla \mathbf{r}(t,x)$ will be justified below.

Before coming to the computation of F, we observe that the last term of the PDE (13) for $\mathbf{r}_K$ may be written as

$$-\alpha\, \mathbf{r}_K(t,x) \int_D \Gamma_y^K(x) \nu^K(dy).$$

Replacing $\nu^K(dy)$ with its limit $u(t,y)dy$ and passing to the limit $K \to +\infty$ would formally give the second equation of (12) with

$$\delta = \frac{\alpha}{\sqrt{2\pi}\, \sigma_{\mathbf{r}}}.$$

However, this requires a sufficient regularity for $u(t,x)$ and a convergence of $\nu_t^K(dy)$ to $u(t,y)dy$ such that space means of ν_t^K over balls of diameter of the order of $K^{-\eta/2}$ also

converge to $u(t,x)$. This is the place where a full mathematical proof requires a careful analysis that we do not examine here.

Finally, we need to compute the distribution of the preferred dispersion direction over the population close to a fixed $x \in \mathcal{D}$ at a fixed time $t \geq 0$. We consider one of these ramets chosen at random and call it RSI (Randomly Sampled Individual) at x, and we divide the computation into several steps.

Scaled age distribution of a RSI

Because of the scaling of the death rate $\mu_K(t,x)$, the life span of the RSI is of order $K^{-\eta}$, and the position of its mother ramet is at a distance of order $K^{-\eta/2}$ because of the scaling of the p.d.f. g. Over these time and space scales, the population densities and resource concentration can be assumed constant equal to $u(t,x)$ and $\mathbf{r}(t,x)$. We call *scaled age* of an individual at x at time t, its age multiplied by K^η.

In particular, the ramets alive at time t close to x appeared at an (approximately) constant rate during a time length of order $K^{-\eta}$. Since they die (approximately) at constant rate $K^\eta\gamma(x)$, the probability of survival of an individual born at time $t - yK^{-\eta}$ is $e^{-y\gamma(x)}$. Since the birth rate of individuals close to x is approximately constant, we deduce that the scaled age of a RSI at x is asymptotically distributed when $K \to +\infty$ as an exponential random variable with parameter $\gamma(x)$.

Number of living offsprings of a RSI

Conditionally on the age $K^{-\eta}y$ (or the scaled age y) of a RSI at x, the birth rate at x over the time interval $[t - K^{-\eta}y, t]$ is (approximately) constant equal to $K^\eta\gamma(x)$. Therefore, the scaled age of all its offspring is distributed as a Poisson process of parameter $\gamma(x)$ on the interval $[0,y]$. In particular, the total number of offsprings is distributed as a Poisson random variable with parameter $y\gamma(x)$. Among them, some are already dead at time t.

In order to compute the number of living neighbors of the RSI, we need to introduce an additional conditioning on the number k of offspring of a RSI conditioned to have scaled age y. We use the following feature of Poisson processes: conditionally of the number k of offspring of the RSI, their scaled age are distributed as k independent and identically distributed (i.i.d.) random variables with uniform distribution on $[0,y]$. In other words,

conditionally on the age $K^{-\eta}y$ of the RSI and the number of its children k, the ages of its children are distributed as k i.i.d. random variable with uniform distribution on $[0, K^{-\eta}y]$.

Since they all die at (approximate) rate $K^{\eta}\gamma(x)$, the survival probability of each is

$$\frac{1}{K^{-\eta}y}\int_0^{K^{-\eta}y} e^{-K^{\eta}\gamma(x)s}ds = \frac{1-e^{-y\gamma(x)}}{y\gamma(x)}.$$

We denote by $p_{x,y}$ the right-hand side of this equation. This leads to a number of living children of the RSI with binomial distribution with parameters k and $p_{x,y}$.

Number of living neighbors of a RSI

Similarly, conditionally on the scaled age y of the RSI, its mother ramet is still alive at time t with probability $e^{-y\gamma(x)}$.

Therefore, the number N of living neighbors of a RSI at x conditionally on $A = y$, where A is the scaled age of the RSI, is distributed as

$$\begin{aligned}\mathbb{P}(N = n \mid A = y) = e^{-y\,\gamma(x)} &\sum_{k\geq n-1} e^{-y\,\gamma(x)}\frac{(y\,\gamma(x))^k}{k!}\binom{k}{n-1}p_{x,y}^{n-1}(1-p_{x,y})^{k-n+1}\\ &+(1-e^{-y\,\gamma(x)})\sum_{k\geq n} e^{-y\,\gamma(x)}\frac{(y\,\gamma(x))^k}{k!}\binom{k}{n}p_{x,y}^{n}(1-p_{x,y})^{k-n},\end{aligned}$$

for $n \geq 1$ and

$$\mathbb{P}(N = 0 \mid A = y) = (1-e^{-y\,\gamma(x)})\sum_{k\geq 0} e^{-y\,\gamma(x)}\frac{(y\,\gamma(x))^k}{k!}(1-p_{x,y})^k.$$

Denoting for convenience these quantities $q_{x,y}(n)$, we obtain the following distribution for the number N of living neighbors of a RSI at x: for all $n \geq 0$,

$$\mathbb{P}(N = n) = \int_0^{+\infty} \gamma(x)e^{-y\,\gamma(x)}\,q_{x,y}(n)\,dy. \tag{16}$$

Positions of the neighbors of a RSI

Neglecting the smaller-order terms in (15), we have

$$D_{t,x}^K \approx \tfrac{1}{K^{\eta}}g\Big(\tfrac{\|v\|}{K^{\eta/2}}\Big)\tfrac{(\mathbf{d}_{t,x},v)}{2\pi},$$

which means that the direction of dispersal is (approximately) uniform for each birth. This is also the case for the births from the RSI at x, as well as its mother ramet. Therefore, the positions of all the neighbors of the RSI at x are i.i.d. and distributed as $x + K^{-\eta/2}\rho v_\theta$, where ρ has p.d.f. $g(\rho)$ and $v_\theta = (\cos\theta, \sin\theta)$.

Asymptotic distribution of $\mathbf{d}_{t,x}$

Since the length of connections is of order $K^{-\eta/2}$, we can replace $\mathbf{r}(t, x_t^i) - \mathbf{r}(t, x)$ with $\nabla\mathbf{r}(t, x) \cdot (x_t^i - x)$ in the formula (9) for the preferred dispersion direction $\mathbf{d}_{t,x}$. Therefore, conditionally on $N = n \geq 1$, the preferred dispersion direction $\mathbf{d}_{t,x}$ of a RSI at x is distributed as

$$\frac{1}{n}\sum_{i=1}^{n}(\nabla\mathbf{r}(t, x) \cdot v_{\theta_i})v_{\theta_i}, \tag{17}$$

where $\theta_1, \theta_2, \ldots$ are i.i.d. random variable uniformly distributed on $[0, 2\pi)$.

Introducing $\theta_{t,x}$ such that $\nabla\mathbf{r}(t, x) = \|\nabla\mathbf{r}(t, x)\|\, v_{\theta_{t,x}}$, and applying the rotation of angle $-\theta_{t,x}$ to the vector (17) yields

$$\frac{1}{n}\sum_{i=1}^{n}\cos(\theta_i')\, v_{\theta_i'}, \tag{18}$$

where the θ_i' are i.i.d. and uniformly distributed on $[0, 2\pi)$.

Denoting by $\mu(w)dw$ the distribution of $\cos(\theta)v_\theta$ for θ uniformly distributed on $[0, 2\pi)$, the distribution of the vector (18) is $\mu^{*n}(nw)\, dw$, where $\mu^{*n} = \mu * \ldots * \mu$ and $*$ denotes the convolution operator. Therefore, a RSI at x at time t has the following distribution for its preferred dispersal direction $\mathbf{d}_{t,x}$ rotated of the angle $-\theta_{t,x}$:

$$\mathbb{P}(N = 0)\, \delta_0(dw) + \sum_{n\geq 1}\mathbb{P}(N = n)\, \mu^{*n}(nw)\, dw$$

where $\mathbb{P}(N = n)$ is given by (16). Denoting by $\pi(dw)$ the previous distribution, we finally obtain

$$F(x, \nabla\mathbf{r}(t, x)) = \langle v_{t,x}\rangle = \int_{\mathbb{R}^2}\pi(dw)\int_0^{2\pi}d\theta\int_0^{+\infty}d\rho\,\rho\, v_{\theta_{t,x}+\theta}\, f\big(\kappa(\|w\|),\, (w, v_\theta)\big)\, g(\rho)\,.$$

Note that the right-hand side only depends on x through the distribution of N, and on $\nabla\mathbf{r}(t, x)$ through the angle $\theta_{t,x}$.

Acknowledgment: We are very grateful to Cendrine Mony who gave us valuable advices and comments on a preliminary version of this work.

References

Bell, A.D., 1979. The hexagonal branching pattern of rhizomes of *Alpinia speciosa* L. (Zingieraceae). Ann. Bot. 43, 209–223.

Bell, A. D., Tomlison, P. B., 1980. Adaptive architecture in rhizomatous plants. Bot. J. Linn. Soc. 80, 125-160.
Birch, D. A., Young, W. R., 2006. A master equation for a spatial population model with pair interactions. Theoretical Population Biology 70 (1), 26–42.
Bolker B. M., 2004. Continuous-space models for population dynamics. In: I. Hansi and O. E. Gaggioti (Eds.), Ecology, Genetics and Evolution of Metapopulations, pp. 45–69. Elsevier Science, San Diego, CA.
Bolker, B. M., Pacala, S. W., 1999. Spatial moment equations for plant competition: understanding spatial strategies and the advantages of short dispersal. American Naturalist 153, 575–602.
Brown, D. H., Bolker, B. M., 2004. The effects of disease dispersal and host clustering on the epidemic threshold in plants. Bulletin of Mathematical Biology 66, 341–371.
Campillo, F., Champagnat, N., 2012. Large population scalings for individual-based stochastic models of graph-structured populations, in preparation.
Campillo, F., Joannides, M., 2009. A spatially explicit Markovian individual-based model for terrestrial plant dynamics. ArXiv Mathematics e-prints (arXiv:0904.3632v1).
Cerf, R, 2006. The Wulff crystal in Ising and Percolation models. Lecture Notes in Mathematics 1878, Springer-Verlag, Berlin.
Champagnat, N., Ferrière, R., Méléard, S., 2006. Unifying evolutionary dynamics: from individual stochastic processes to macroscopic models. Theoretical Population Biology 69 (3), 297–321.
Champagnat, N., Ferrière, R., Méléard, S., 2008. From individual stochastic processes to macroscopic models in adaptive evolution. Stochastic Models 24, Suppl. 1, 2–44.
Champagnat, N., Méléard, S., 2011. Polymorphic evolution sequence and evolutionary branching. Probability Theory and Related Fields 151 (1), 45–94.
Charpentier, A., Stuefer, J. F., 1999. Functional specialization of ramets in *Scirpus maritimus*. Plant Ecology 141, 129–136.
Cheplick, G. P., 1997. Responses to severe competitive stress in a clonal plant: differences between genotypes. Oikos 79:581–591.
DeAngelis, D. L., Gross, L. J. (Eds.), 1992. Individual-based models and approaches in ecology: populations, communities and ecosystems. Chapman and Hall.
Dieckmann, U., Herben, T., Law, R., 1999. Spatio-temporal processes in ecological communities. CWI Quarterly 12, 213–238.
Dieckmann, U., Law, R., May 1996. The dynamical theory of coevolution: a derivation from stochastic ecological processes. Journal of Mathematical Biology 34 (5), 579–612.
Dieckmann, U., Law, R., Metz, J. A. J. (Eds.), 2000. The Geometry of Ecological Interactions: Simplifying Spatial Complexity. Cambridge University Press.
Durrett, R., 1995. Ten lectures on particle systems. In: Lectures on Probability Theory (Saint Flour, 1993). Lecture Notes in Mathematics 1608, pp. 97–201. Springer-Verlag, Berlin.
El Hamidi, A., Garbey, M., Ali, N., 2012. On nonlinear coupled diffusions in competition systems. Nonlinear Analysis: Real World Applications 13(3), 1306–1318.
Etheridge, A. M., 2004. Survival and extinction in a locally regulated population. Annals of Applied Probability 14 (1), 188–214.
Fournier, N., Méléard, S., 2004. A microscopic probabilistic description of a locally regulated population and macroscopic approximations. Annals of Applied Probability 14, 1880–1919.
Grimm, V., Railsback, S. F., 2005. Individual-based Modeling and Ecology. Princeton University Press.
Harper, J. L., 1981. The concept of the modular organism. In R. M. May (ed.), Theoretical ecology: Principles and applications, 2nd edn. Sinauer, Sunderland: 53–77.
Hartig, F., Calabrese, J. M., Reineking, B., Wiegand, T., Huth, A., 2011. Statistical inference for stochastic simulation models – theory and application. Ecol. Lett. 14(8), 816–827.
Herben, T., Novoplansky, A., 2008. Implications of self/non-self discrimination for spatial patterning of clonal plants. Evol. Ecol. 22, 337–350.
Herben, T., Suzuki, J.-I., 2002. A simulation study of the effects of architectural constraints and resource translocation on population structure and competition in clonal plants. Evolutionary Ecology 15, 403–423.
Humphrey, L.D., Pyke, D.A., 1997. Clonal foraging in perennial wheatgrasses - A strategy for exploiting patchy soil nutrients. Journal of Ecology, 85 (5), 601–610.
Humphrey, D.L., Pyke, D.A., 1998. Demographic and growth responses of a guerrilla and a phalanx perennial grass in competitive mixtures. Journal of Ecology 86 (5), 854–865.
Hutchings, M. J., 1999. Clonal plants as cooperative systems: benefits in heterogeneous environments. Plant Species Biology 14, 1–10.

Kisljuk, O.S., Kusnetzova, T.V., Agafonova, A.A., 1996. On the modeling of clone geometry in *Asarum europaeum*. J. Theor. Biol. 178, 399–404.

Kipnis, C., Landim, C., 1999. Scaling limits of interacting particle systems. Springer-Verlag, Berlin.

Klimeš, L., Klimešova, J., Hendriks, R. J. J., van Groenendael, J., 1997. Clonal plants architectures: a comparative analysis of form and function. In: de Kroon, H., van Groenendale, J. (Eds.), The Ecology and Evolution of Clonal Plants. Backhuys Publishers, Leiden, pp. 1–29.

Kun, Á., Oborny, B., 2003. Survival and competition of clonal plant populations in spatially and temporally heterogeneous habitats. Community Ecology 4, 1–20.

Lovett-Doust L. 1981. Population dynamics and local specialization in a clonal perennial (Ranunculus repens). Journal of Ecology 69: 743–755.

Marshall, C., 1990. Source–sink relations of interconnected ramets. In J. van Groenendael and H. de Kroon (Eds.) Clonal Growth in Plants: Regulation and Function. SPB Academic Publishing, The Hague, pp. 23–41.

Méléard, S., Tran, V. C., 2009. Trait substitution sequence process and canonical equation for age-structured populations. Journal of Mathematical Biology 58 (6), 881–921.

Metz, J. A. J., Geritz, S. A. H., Meszéna, G., Jacobs, F. J. A., van Heerwaarden, J. S., 1996. Adaptive dynamics, a geometrical study of the consequences of nearly faithful reproduction. In: Stochastic and spatial structures of dynamical systems (Amsterdam, 1995). Konink. Nederl. Akad. Wetensch. Verh. Afd. Natuurk. Eerste Reeks, 45. North-Holland, Amsterdam, pp. 183–231.

Mony, C., Garbey, M., Smaoui, M., Benot, M. L., 2012. Large Scale Parameter Study of an Individual Based Model of Clonal Plant with Volunteer Computing. To appear in Ecological Modelling.

Novoplansky, A., 2009. Picking battles wisely: plant behaviour under competition. Plant Cell Environ. 32, 726–741.

Oborny, B., 1994. Growth rules in clonal plants and environmental predictability – a simulation study. Journal of Ecology 82, 341–351.

Oborny, B., Czárán, T., Kun, Á., 2001. Exploration and exploitation of resource patches by clonal growth: a spatial model on the effect of transport between modules. Ecological Modelling 141, 151–169.

Oborny, B., Englert, P., 2012. Plant growth and foraging for a patchy resource: A credit model. To appear in Ecological Modelling.

Oborny, B., Kun, A., 2002. Fragmentation of clones: how does it influence dispersal and competitive ability? Evolutionary Ecology 15, 319–346.

Oborny, B., Kun, Á., Czárán, T., Bokros, S., 2000. The effect of clonal integration on plant competition for mosaic habitat space. Ecology 81, 3291–3304.

Smith, A. P., Palmer, J. O. 1976, Vegetative reproduction and close packing in a successional plant species. Nature 261, 232–23.

Stuefer, J., Gomez, S., Van Mölken, T., 2004. Clonal integration beyond resource sharing: implications for defence signalling and desease transmission in clonal plant networks. Evolutionary Ecology 18, 647—667.

van Groenendael, J.M., Kliměs, L., Kliměsová, J., Hendricks, R.J.J., 1996. Comparative ecology of clonal plants. Philos Trans. R. Soc. Lond. B 351, 1331–1339.

van Kleunen, M., Fischer, M., 2001. Adaptive evolution of plastic foraging responses in a clonal plant. Ecology 82(12), 3309–3319

Wijesinghe, D. K., Hutchings, M. J., 1997. The effects of spatial scale of environmental heterogeneity on the growth of clonal plant: An experimental study with *Glechoma hederacea*. Journal of Ecology 85, 17–28.

Wildovà, R., Gough, L., Herben, T., Hershock, C., Goldberg, D., 2007. Architectural and growth traits differ in effects on performance of clonal plants: an analysis using a field-parameterized simulation model. Oikos 116, 836–852.

Winkler, E., Fischer, M., 2002. The role of vegetative spread and seed dispersal for optimal life histories of clonal plants: a simulation study. Evolutionary Ecology 15 (4-6), 1573–8477.

Winkler, E., Fischer, M., Schmid, B., 1999. Modelling the competitiveness of clonal plants by complementary analytical and simulation approaches. Oikos 85, 217–233.

Winkler, E., Klotz, S., 1997. Clonal plant species in a dry-grassland community: A simulation study of long-term population dynamics. Ecological Modelling 96 (1-3), 125 – 141.

Winkler, E. and Schmid, B., 1995. Clonal strategies of herbaceous plant species - a simulation study on population growth and competition. Abstracta Bot., 19: 17-28.

Winkler, E., Stöcklin, J., 2002. Sexual and vegetative reproduction of Hieracium pilosella L. under competition and disturbance: a grid-based simulation model. Annals of Botany 89, 525–536.

Wong, S., Anand, M., Bauch, C.T., 2011. Agent-based modelling of clonal plant propagation across

space: recapturing fairy rings and other real-world phenomena. Ecological Informatics 6: 127-135.